J|A|C|S
COMMUNICATIONS

Published on Web 09/09/2003

Molecular Imprinting of Biomineralized CdS Nanostructures: Crystallographic Control Using Self-Assembled DNA−Membrane Templates

Hongjun Liang, Thomas E. Angelini, James Ho, Paul V. Braun, and Gerard C. L. Wong*

Department of Materials Science and Engineering and Department of Physics, University of Illinois at Urbana-Champaign, Urbana, Illinois 61801

Received June 5, 2003; E-mail: gclwong@uiuc.edu

A wide range of biomineralization[1] and templating[2,3] methods exist for organizing inorganic materials at a wide range of length-scales. Here, we show that crystallographic control of the inorganic nanostructures is possible using synthetic biomolecular templates comprised of anionic DNA and cationic membranes,[4] which self-assemble into a multilamellar structure where a periodic one-dimensional (1D) lattice of parallel DNA chains is confined between stacked two-dimensional (2D) lipid sheets. We have organized Cd^{2+} ions within the interhelical pores between DNA strands and subsequently reacted them with H_2S to form CdS nanorods of controllable widths and crystallographic orientation. The strong electrostatic interactions align the templated CdS (002) polar planes parallel to the negatively charged sugar−phosphate DNA backbone, which indicates that molecular details of the DNA molecule are imprinted onto the inorganic crystal structure. The resultant nanorods have (002) planes tilted by 60° with respect to the rod axis, in contrast to all known II−VI semiconductor nanorods.[5]

Lamellar DNA−cationic membrane complexes, originally conceived for gene therapy, are examples of a new class of hierarchically organized nanoporous biopolymer−membrane systems.[4,6] As the membrane charge density is changed at the isoelectric point, the inter-DNA spacing can be controlled between 2.5 and 5.7 nm.[4] Liposomes comprised of binary mixtures of the neutral lipid DOPC (dioleoyl-phosphatidylcholine) and cationic lipid DOTAP (dioleoyl-trimethylammonium propane) are mixed with an aqueous DNA solution to form the self-assembled complexes. Two different types of DNA have been used, λ-phage DNA (48,502 base pairs, contour length 16.5 μm) and polydisperse calf thymus DNA, with essentially the same results. The structure of a typical isoelectric lamellar complex at a DOTAP/DOPC mass ratio of 70/30 at low global divalent counterions concentration is illustrated by the synchrotron small-angle X-ray scattering (SAXS) data in Figure 1a, which shows the two harmonics of scattering from the lamellar ordering at $q_1 = 0.099$ Å^{-1} and $q_2 = 0.198$ Å^{-1}, and corresponds to a d spacing of $d_c = 6.35$ nm, consistent with the thickness of a membrane layer plus a hydrated DNA diameter. The inter-DNA correlation (marked by arrow) can be clearly seen at $q_{DNA} = 0.183$ Å^{-1}, corresponding to an inter-DNA spacing of $d_{DNA} = 3.43$ nm.

DNA within these lamellar complexes can condense in the presence of divalent counterions into close-packed rafts.[7] As the concentration of Cd^{2+} is increased, via the addition of $CdCl_2$, the DNA strands undergo a dramatic 2D condensation, which is evidenced by the reduction in inter-DNA spacing (marked by arrow, $d_{DNA} \approx 2.65$ nm, Figure 1b). This spacing is slightly smaller than the hydrated DNA diameter (~2.5 nm) plus a hydrated Cd^{2+} ion diameter (~0.4 nm) and suggests the existence of confined Cd^{2+} ions between the DNA strands, which partially neutralize the DNA negative charge.[7] Because the DNA−membrane complex precipitates out of solution, the Cd^{2+} concentration within the complexes can be inferred by measuring the characteristic Cd emission intensity

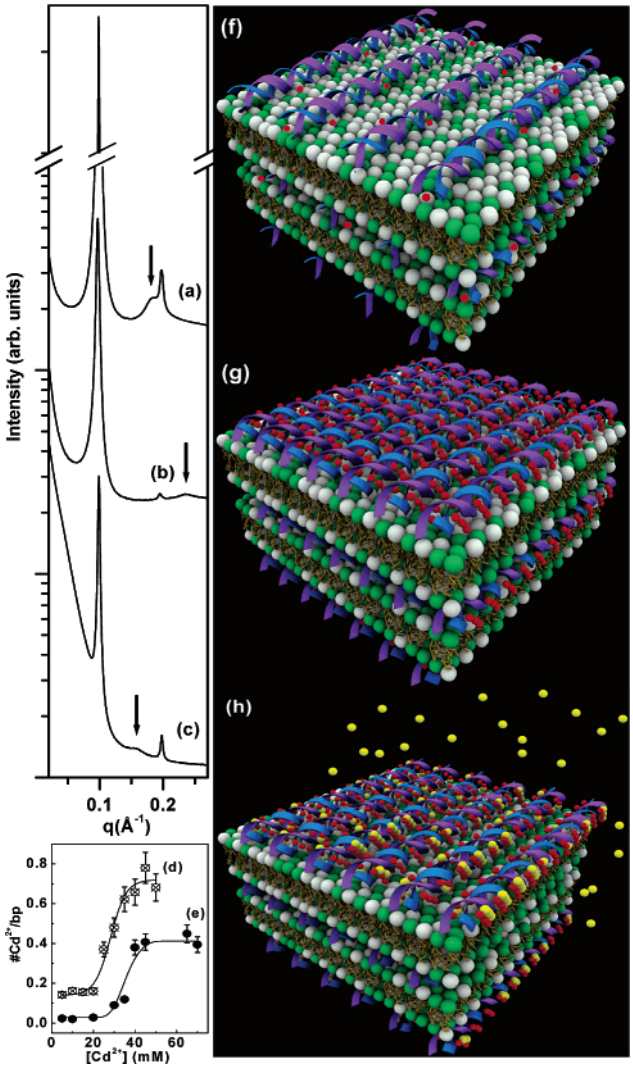

Figure 1. Structural evolution of DNA−membrane templates during biomineralization of CdS: (a) $[Cd^{2+}] = 10$ mM; (b) $[Cd^{2+}] = 40$ mM; (c) $[Cd^{2+}] = 40$ mM, after reaction with H_2S. Note changes in the inter-DNA spacing (arrow). Cd^{2+} ions density inside isoelectric calf thymus DNA−membrane templates for DOTAP/DOPC = 30/70 (d), and DOTAP/DOPC = 70/30 (e), as measured by ICPS. The schematic pictures in (f), (g), and (h) indicate membrane−DNA template organization from the SAXS data. The Cd^{2+} ions (red balls) are organized by DNA strands (blue-purple) in the lamellar complexes and subsequently react with H_2S (yellow balls) to form CdS.

of the supernatant using inductively coupled plasma spectroscopy (ICPS). The intracomplex Cd^{2+} ion concentration is drastically increased at the global Cd^{2+} concentration at which the DNA strands condense (Figure 1d,e). Interestingly, the number of condensed Cd^{2+} ions within the complex required for 2D DNA condensation

10.1021/ja036529o CCC: $25.00

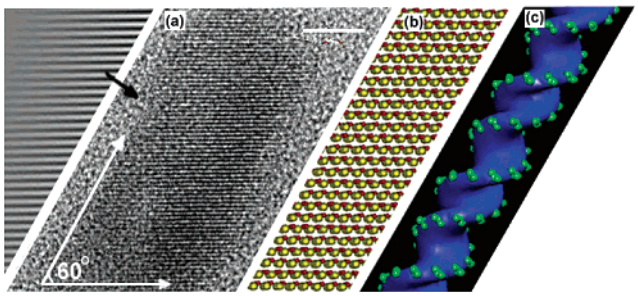

Figure 2. (a) HRTEM of a typical templated CdS nanorod (scale bar is 5 nm): Note tilt of (002) planes relative to rod axis. (b) Schematic representation of crystal structure within nanorod (Cd, red; S, yellow) showing (002) planes. (c) Schematic representation of B-form DNA, showing the negatively charged phosphate groups (green) on the backbone, which organize the Cd^{2+} ions and guide the nucleation of CdS.

increases as the membrane charge density decreases: For isoelectric complexes with DOTAP/DOPC = 70/30, approximately 0.4 Cd^{2+} ions are condensed with each DNA base pair (Figure 1e), whereas for complexes with DOTAP/DOPC = 30/70, the number is 0.7 Cd^{2+} ions per base pair (Figure 1d).

The condensed Cd^{2+} ions within the DNA−membrane complexes can be reacted with gaseous H_2S to form CdS. The peak positions and peak widths from wide-angle X-ray scattering (WAXS) of the complexes after H_2S reaction confirm the existence of nanoscopic wurtzite CdS (Supporting Information). The structural evolution of isoelectric cationic lipid−DNA complexes during growth of CdS has been monitored using SAXS. The structure of the postgrowth DNA−membrane complex is indicated in Figure 1c. The inter-DNA spacing has expanded by ∼1.3 nm, likely due to a combination of CdS nanorod growth and the resultant neutralization of Cd^{2+} ions. Because the density of Cd^{2+} ions within the complexes is small as compared to that in crystalline CdS, this suggests that isolated CdS nanorods have grown along the DNA strands. The lamellar spacing remains approximately constant and suggests that the biomolecular structure is robust during the templating process.

The CdS grown within the DNA−membrane complexes can be isolated by dissolving the charged biomolecular components in a 1% sodium dodecyl sulfate (SDS) solution. The solution-dispersed CdS is cast onto a holey carbon grid and imaged using transmission electron microscopy (TEM). The width of the templated CdS nanorods decreases with increasing membrane charge density, which is consistent with the observed trend in the initial number of condensed Cd^{2+} ions from the ICPS measurement. For isoelectric complexes with DOTAP/DOPC = 70/30, the CdS rod widths are 5 ± 1 nm, whereas for complexes with DOTAP/DOPC = 30/70, the rod widths are 10 ± 1 nm.

Current techniques for wurtzite structure II−VI semiconductor nanorod growth exploit the anisotropic growth rates for different lattice planes; hence, the rod direction is perpendicular to the (002) planes.[5] Surprisingly, nanorods grown from the DNA−membrane complexes are not oriented along the *c*-axis. This is clearly seen in the high-resolution TEM (HRTEM) image of a representative single nanorod (Figure 2a), templated from isoelectric complexes of calf thymus DNA with DOTAP/DOPC = 30/70 at $[Cd^{2+}]$ = 40 mM. A 2× magnified Fourier filtered image is also shown to the left of Figure 2a. The lattice fringes correspond to (002) planes of CdS (d = 0.336 nm), which are tilted by 60° from the rod axis. A schematic representation of the wurtzite CdS arrangement within the nanorod is shown in Figure 2b.

This observed tilt of the (002) lattice planes can be related to the orientation of the DNA sugar−phosphate backbone, which is tilted by ∼60° with respect to the helix axis in B-form DNA when projected onto a 2D plane[8] (Figure 2c). The spatial distribution of the positively charged Cd^{2+} ions, and therefore the nucleation of the CdS polar (002) planes, is organized by this negatively charged "ridge" on the DNA surface (Figure 1h). Because the templated CdS nanorods are confined between DNA strands, the (002) planes are tilted by ∼60° with respect to the nanorod major axis. Interestingly, the periodicity of each helical turn of B-form DNA is ∼3.4 nm, which is just enough to fit 10 (002) planes with nearly no mismatch.

In conclusion, we achieved crystallographic control in biomineralized inorganic nanostructures, by employing a form of molecular imprinting using a synthetic, biomolecular template comprised of anionic and cationic components. The use of strong electrostatic interactions in this context can potentially lead to new possibilities in supramolecular self-assembly and nanocrystal engineering.

Acknowledgment. This work was supported in part by NSF-DMR-0071761, the NSF Nanoscience & Engineering Initiative, the Petroleum Research Fund, the Beckman Young Investigator Program, and the U.S. Department of Energy, Division of Materials Sciences under Award No. DEFG02-91ER45439 through the Frederick Seitz Materials Research Laboratory and the Center for Microanalysis of Materials at UIUC. We are also grateful to Dr. Jianguo Wen and Prof. Jianmin Zuo for help with TEM.

Supporting Information Available: Reaction schematic, WAXS, and low-magnification TEM data (PDF). This material is available free of charge via the Internet at http://pubs.acs.org.

References

(1) (a) Addadi, L.; Weiner, S. *Angew. Chem., Int. Ed. Engl.* **1992**, *31*, 153−169. (b) Monnier, A.; Schuth, F.; Huo, Q.; Kumar, D.; Margolese, D.; Maxwell, R. S.; Stucky, G. D.; Krishnamurty, M.; Petroff, P.; Firouzi, A.; Janicke, M.; Chmelka, B. F. *Science* **1993**, *261*, 1299−1303. (c) Aizenberg, J.; Tkachenko, A.; Weiner, S.; Addadi, L.; Hendler, G. *Nature* **2001**, *412*, 819−822. (d) Mann, S. *Biomineralization: Principles and Concepts in Bioinorganic Materials Chemistry*; Oxford University Press: New York, 2002. (e) Whaley, S. R.; English, D. S.; Hu, E. L.; Barbara, P. F.; Belcher, A. M. *Nature* **2000**, *405*, 665−668. (f) Hartgerink, J. D.; Beniash, E.; Stupp, S. I. *Science* **2001**, *294*, 1684−1688.

(2) (a) Kresge, C. T.; Leonowicz, M. E.; Roth, W. J.; Vartuli, J. C.; Beck, J. S. *Nature* **1992**, *359*, 710−712. (b) Murray, C. B.; Kagan, C. R.; Bawendi, M. G. *Science* **1995**, *270*, 1335−1338. (c) Brinker, C. J. *Curr. Opin. Colloid Interface Sci.* **1998**, *3*, 166−173. (d) Attard, G. S.; Bartlett, P. N.; Coleman, N. R. B.; Elliott, J. M.; Owen, J. R.; Wang, J. H. *Science* **1997**, *278*, 838−840.

(3) (a) Braun, P. V.; Stupp, S. I. *Science* **1997**, *277*, 1242−1248. (b) Braun, P. V.; Osenar, P.; Stupp, S. I. *Nature* **1996**, *380*, 325−328. (c) Shenton, W.; Pum, D.; Sleytr, U. B.; Mann, S. *Nature* **1997**, *389*, 585−587.

(4) (a) Radler, J. O.; Koltover, I.; Salditt, T.; Safinya, C. R. *Science* **1997**, *275*, 810−814. (b) Koltover, I.; Salditt, T.; Radler, J. O.; Safinya, C. R. *Science* **1998**, *281*, 78−81.

(5) (a) Peng, X. G.; Manna, L.; Yang, W. D.; Wickham, J.; Scher, E.; Kadavanich, A.; Alivisatos, A. P. *Nature* **2000**, *404*, 59−61. (b) Manna, L.; Scher, E. C.; Li, L.-S.; Alivisatos, A. P. *J. Am. Chem. Soc.* **2002**, *124*, 7136−7145. (c) Duan, X.; Lieber, C. M. *Adv. Mater.* **2000**, *12*, 298−302.

(6) Wong, G. C. L.; Tang, J. X.; Lin, A.; Li, Y.; Janmey, P. A.; Safinya, C. R. *Science* **2000**, *288*, 2035−2039.

(7) Koltover, I.; Wagner, K.; Safinya, C. R. *Proc. Natl. Acad. Sci. U.S.A.* **2000**, *97*, 14046−14051.

(8) Sinden, R. R. *DNA Structure and Function*; Academic Press: New York, 1994.

JA036529O